



OPEN

SUBJECT AREAS:
GEOCHEMISTRY
PETROLOGYReceived
21 January 2014Accepted
14 May 2014Published
17 June 2014Correspondence and
requests for materials
should be addressed to
S.C.H. (huang17@fas.
harvard.edu; huangs@
alum.mit.edu)Missing Lead and High $^3\text{He}/^4\text{He}$ in
Ancient Sulfides Associated with
Continental Crust FormationShichun Huang¹, Cin-Ty A. Lee² & Qing-Zhu Yin³¹Department of Earth and Planetary Sciences, Harvard University, ²Department of Earth Science, Rice University, ³Department of Earth and Planetary Sciences, University of California, Davis.

Major terrestrial reservoirs have Pb isotopes more radiogenic than the bulk silicate Earth. This requires a missing unradiogenic Pb reservoir, which has been argued to reside in the lower continental crust or dissolved in the core. Chalcophile element studies indicate that continent formation requires the formation of sulfide-bearing mafic cumulates in arcs. Because Pb, but not U, partitions into sulfides, we show that continent formation must have simultaneously generated time-integrated unradiogenic Pb reservoirs composed of sulfide-bearing cumulates, now recycled back into the mantle or stored deep in the continental lithosphere. The generation of such cumulates could also lead to coupled He-Pb isotopic systematics because ^4He is also produced during U-Th-Pb decay. Here, we show that He may be soluble in sulfide melts, such that sulfide-bearing cumulates would be enriched in both Pb and He relative to U and Th, “freezing” in He and Pb isotopes of the ambient mantle at the time of sulfide formation. This implies that ancient sulfide-bearing cumulates would be characterized by unradiogenic Pb and He isotopes (high- $^3\text{He}/^4\text{He}$). These primitive signatures are usually attributed to primordial, undifferentiated mantle, but in this case, they are the very imprint of mantle differentiation via continent formation.

The geochemical behavior of Pb in the Earth is not fully understood. Most upper crustal and upper mantle reservoirs have Pb isotopes more radiogenic than bulk Earth estimates, manifested by silicate reservoirs plotting to the right of the geochron on a $^{206}\text{Pb}/^{204}\text{Pb}$ versus $^{207}\text{Pb}/^{204}\text{Pb}$ diagram. This imbalance, known as the “Pb paradox”, means that a missing reservoir with unradiogenic Pb is required to balance the radiogenic Pb¹. One solution is that the missing unradiogenic Pb resides in the present-day lower continental crust². However, most lower crustal xenoliths are not sufficiently unradiogenic to satisfy this mass balance^{3,4,5}. Another hypothesis, motivated by experimental studies, is that Pb dissolved into the Earth’s core early in Earth’s history^{6,7}. If Pb indeed segregated into the core, the U-Pb systematics of the bulk silicate Earth would indicate that the core formed 80–140 Myr after planetary accretion^{6,7}, but this core formation age is much later than the <30 Myr after accretion based on ^{182}Hf - ^{182}W isotopic systematics, which is uniquely sensitive to core formation^{8,9} (unlike the U-Pb system, which can be fractionated by processes unrelated to core formation). Alternatively, this young U-Pb age of the bulk silicate Earth, 80–140 Myr after Earth’s accretion^{6,7}, has been used to argue for a late accretion of volatile elements, such as Pb, to the Earth^{10,11}. Due to these inconsistencies, additional hypotheses should be explored.

Sulfide minerals are another potentially important carrier of Pb¹². A recent study by Lee et al.¹³ showed that pyroxenite cumulates formed during the differentiation of arc magmas are enriched in sulfides and therefore enriched in strongly chalcophile (sulfide-loving) elements like Cu. The bulk continental crust is felsic in composition because a large amount of mafic cumulates were formed and then removed from the continental crust by delamination^{14,15}. Lee et al.¹³ showed that the Cu content of the continental crust is depleted relative to basaltic magmas and even the mantle, which implies that the complementary mafic cumulates should be sulfide-bearing.

The amount of S, in the form of sulfide, which must be missing from the continental crust, can be evaluated by considering the compositional effects on sulfide solubility during magmatic differentiation. Assuming the initial building blocks of continents are basalts and that almost all basalts are sulfide-saturated in their mantle source regions, the initial S contents of these juvenile basalts will range from 1600–2000 ppm¹⁶. Because sulfide solubility decreases substantially with increasing SiO_2 and decreasing FeO contents, by the time the basalts evolve to andesitic compositions typical of bulk continental crust, the S content at sulfide solubility has fallen to <200 ppm¹⁶ (solubility may rise with further magmatic evolution if oxygen fugacities rise, but it is the andesitic compositions that are of interest here as such compositions most closely match the average composition of the



continental crust). Based on the foregoing analysis, possibly ~90% of the original S must be either sequestered in the form of sulfide-bearing cumulates or lost during volcanic degassing^{17,18}, leaving behind a S-depleted continental crust¹³.

The presence of a sulfide-bearing mafic reservoir, a required by-product of continent formation, has important implications for Pb. Pb is a moderately chalcophile element. Depending on the Pb partition coefficient in sulfide (14–40)¹², these sulfide-rich cumulates may sequester 5–15% of the parental magma's Pb, the rest remaining in the continental crust¹³. Because these sulfide-bearing cumulates sequester negligible amounts of U and Th, they would be expected to “freeze” in the Pb isotopic composition of the mantle at the time of their formation, generating a reservoir for unradiogenic Pb. In fact, unradiogenic Pb isotopic compositions, plotting on the left side of the geochron in a $^{206}\text{Pb}/^{204}\text{Pb}$ vs. $^{207}\text{Pb}/^{204}\text{Pb}$ diagram, have been found in sulfide inclusions from abyssal peridotites in the Atlantic Ocean¹⁹.

To explore this hypothesis further, we turn to He because ^4He is also a decay product of U–Th–Pb alpha-decay systems. Sulfides formed during magmatic differentiation are likely to be initially in the liquid state due to their low melting temperatures²⁰. The question arises as to whether noble gases like He might be soluble in sulfide liquids. As long as there is a finite solubility of He in sulfide liquids, regardless of how small, and because U and Th do not partition at all into sulfides, we hypothesize that sulfides could effectively “freeze” in the He isotopic compositions of the mantle at the time of formation. If formed early in the Earth's history, these sulfides would be characterized by low $^{206}\text{Pb}/^{204}\text{Pb}$ and high $^{207}\text{Pb}^*/^{206}\text{Pb}^*$ (the ratio of radiogenic ingrowth of ^{207}Pb and ^{206}Pb since the formation of the Earth²¹, and defined as $^{207}\text{Pb}^*/^{206}\text{Pb}^* = (^{207}\text{Pb}/^{204}\text{Pb} - 10.297)/(^{206}\text{Pb}/^{204}\text{Pb} - 9.307)$) and $^3\text{He}/^4\text{He}$, thus Pb–He isotope systematics should be coupled if sulfide control is important, generating negative $^{206}\text{Pb}/^{204}\text{Pb}$ – $^3\text{He}/^4\text{He}$ and positive $^{207}\text{Pb}^*/^{206}\text{Pb}^*$ – $^3\text{He}/^4\text{He}$ correlations. It is thus worth evaluating whether He is soluble in sulfide liquids.

Noble gas studies of sulfides provide some insight. Using step-heated degassing experiments, Yang and Anders²² showed that 30–70% of the total noble gas budget of FeS sulfides is housed in the high temperature fraction, suggesting that noble gases can dissolve directly into the sulfide structure. Given that sulfide liquids are less dense and hence likely to contain more atom-scale void space than sulfide minerals, the fact that small amounts of noble gases can dissolve into the structure of sulfide minerals suggests that noble gases could be even more soluble in liquid sulfides than sulfide minerals.

The solubility of noble gases in basaltic melts has been experimentally investigated^{23,24}, but as far as we know, there are no solubility experiments of noble gases in sulfide liquids. For this reason, we attempt here to infer He solubilities indirectly. Carroll and Stolper²⁵ showed experimentally that the noble gas solubilities in silicate melts correlate well with ionic porosity, allowing them to predict solubilities for those noble gases that have not been studied in detail. Unfortunately, we are unable to apply this method to sulfide melts because a completely different and unknown parameterization is needed given the stronger covalent bonding seen in sulfides than in the metal sites of silicate melts. We thus adopt a different approach based on the work of Uhlig²⁶, Blander et al.²⁷ and Lux²⁴. Assuming that He, being a non-polarizable noble gas, does not interact with the liquid solvent, the free energy change associated with dissolution should be related to the surface energy of the void created by the gas^{26,27}. Taking the macroscopic surface tension γ (mJ/m²) as an approximation of the surface energy associated with the void, the solubility of a noble gas in a liquid has been shown semi-empirically

to follow the following relationship: $\ln \frac{C_{\text{melt}}}{C_{\text{gas}}} = \frac{-4\pi r^2 \gamma N_A}{RT}$, where

the ratio within the logarithm is equivalent to Henry's law constant, N_A is Avogadro's number, R is the gas constant, T is temperature (K), and r is the atomic radius of the noble gas, which we take as an

approximation of the size of the void. Consequently, the partitioning between sulfide and basaltic melts has the following relationship:

$$D_{\text{He}}^{\text{sf/sil}} = \frac{C_{\text{sf}}}{C_{\text{sil}}} = \exp \left[\frac{-4\pi r^2 N_A}{RT} (\gamma_{\text{sf}} - \gamma_{\text{sil}}) \right],$$

where C_{sf} and C_{sil} are the noble gas concentrations in sulfide and basaltic melts and γ_{sf} and γ_{sil} are the macroscopic surface tensions of sulfide and basaltic melts. Using the radius of a He atom (1.08 Å) in six-fold coordination²⁸ and surface tensions of ~370 mJ/m² and ~550 mJ/m² for basaltic and sulfide melts at $T = 1300^\circ\text{C}$ ²⁹, $D_{\text{He}}^{\text{sf/sil}}$ is estimated to be ~0.3. It has been shown that if small amounts of O are dissolved in the sulfide melt, as would be expected at the oxygen fugacity conditions typical of the uppermost mantle (near the quartz-fayalite-magnetite buffer), the wetting angle and by implication the surface tension of a sulfide melt decreases considerably³⁰. This would decrease the difference between sulfide and basaltic melt surface tensions, driving $D_{\text{He}}^{\text{sf/sil}}$ towards greater values.

Because He is almost perfectly incompatible in silicate minerals³¹, most of the He budget within a partially molten system will be contained in the melt phases. Thus, a $D_{\text{He}}^{\text{sf/sil}}$ value of 0.3 or higher implies that non-trivial amounts of He can dissolve in sulfide melts. If sulfide melts, owing to their high densities compared to basaltic melts, can be efficiently segregated from basaltic melts, these sulfide melts become reservoirs characterized by low (U + Th)/He and (U + Th)/Pb because neither U nor Th partitions into sulfides¹². Such sulfide melts can be sealed as inclusions in pyroxenes and olivines that form the mafic cumulates. Since He is insoluble in the host silicate mineral³¹, once the sulfide liquid is trapped, He is unlikely to escape the inclusion, even if sulfide liquids crystallize into sulfide minerals and temperatures remain high enough for He to diffuse rapidly (akin to silicate minerals being entombed as inclusions in diamond and preserving their isotopic signatures). In summary, we speculate that sulfide inclusions in mafic cumulates freeze in the $^3\text{He}/^4\text{He}$, $^{206}\text{Pb}/^{204}\text{Pb}$ and $^{207}\text{Pb}^*/^{206}\text{Pb}^*$ of the ambient mantle at the time of formation. This has important implications for the isotopic evolution of these cumulates.

We now model the secular evolution of $^{206}\text{Pb}/^{204}\text{Pb}$, $^{207}\text{Pb}^*/^{206}\text{Pb}^*$ and $^3\text{He}/^4\text{He}$ in the mantle for closed system and continuous degassing (Fig. 1). As an upper bound on the effect of He degassing, we only consider constant He degassing rate scenarios. During degassing, only He, but not U, Th or Pb, is allowed to leave the system (e.g., into the atmosphere) because U, Th and Pb transported to the crust are then recycled to the mantle, and thus remain within the condensed part of the Earth. The initial $^3\text{He}/^4\text{He}$ is taken as 120 R/Ra³² so that the hypothetical present-day primitive mantle has a $^3\text{He}/^4\text{He}$ of 54 R/Ra (Fig. 1c). The co-evolution of He and Pb isotopic compositions should thus form a negative $^{206}\text{Pb}/^{204}\text{Pb}$ – $^3\text{He}/^4\text{He}$ trend and a positive $^{207}\text{Pb}^*/^{206}\text{Pb}^*$ – $^3\text{He}/^4\text{He}$ trend, the steepness of the slope depending on the integrated extent of degassing (Figs. 1, 2). Losing 98.5% of the primordial ^3He from the Earth's interior results in the present-day MORB $^3\text{He}/^4\text{He}$ value of 8 R/Ra. For comparison, the highest $^3\text{He}/^4\text{He}$ ever found on the Earth (in Baffin Island picrites) is 50 R/Ra³³, which requires almost no degassing or that the He isotopic composition of the mantle was frozen in billions of years ago (Fig. 2). Mathematically, our model for $^3\text{He}/^4\text{He}$ evolution of partially degassed primitive mantle is similar to those discussed elsewhere^{34–37}, but our model is the first that may provide a clear link between He–Pb isotopic evolution and the differentiation of continental crust.

We compiled Pb and He isotopic data from 16 oceanic island basalt (OIB) and continental flood basalt (CFB) localities in Fig. 2 and Table S2. Within individual OIB–CFB suites, He and Pb isotopes appear to be decoupled, most likely because OIB–CFB magmas are mixtures between endmembers having vastly different He/Pb ratios due to previous or contemporaneous degassing events³⁸. The global OIB–CFB data display a boot-shape distribution in a $^{206}\text{Pb}/^{204}\text{Pb}$ vs. $^3\text{He}/^4\text{He}$ plot, but the average of each OIB–CFB suite shows negative

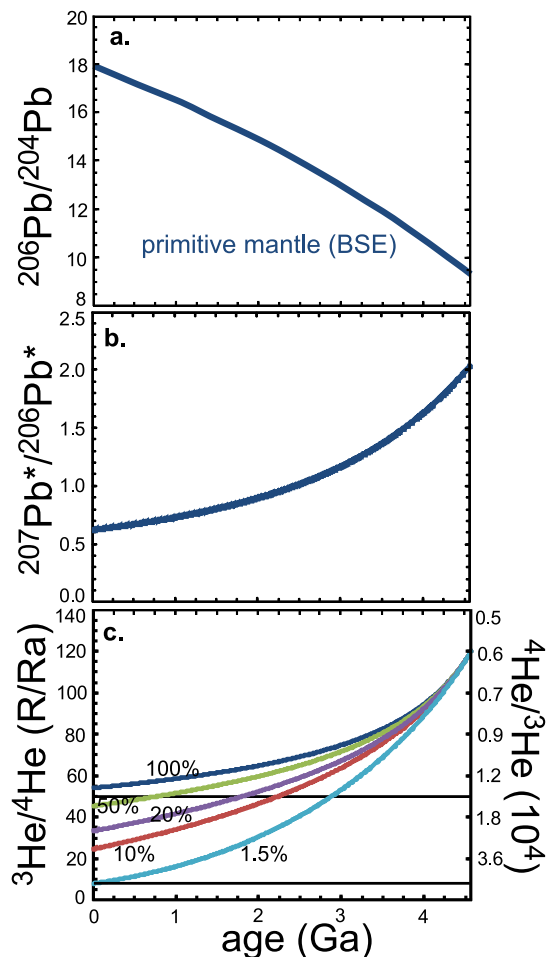


Figure 1 | Time evolution of the primitive mantle and a series of partially degassed primitive mantle reservoirs. For the primitive mantle, the following initial values (at 4.567 Ga, all atomic ratios) are used: $^{238}\text{U}/^{204}\text{Pb} = 16.96$, $^{232}\text{Th}/^{204}\text{Pb} = 41.29$, $^3\text{He}/^{204}\text{Pb} = 0.0215$, $^3\text{He}/^4\text{He} = 1.66 \times 10^{-4}$, and $^{206}\text{Pb}/^{204}\text{Pb} = 9.307$, so that at present-day, the primitive mantle has $^{238}\text{U}/^{204}\text{Pb} = 8.35$ and $^3\text{He}/^4\text{He} = 54 \text{ R/Ra}$. For partially degassed primitive mantle reservoirs, only He, but not U, Th or Pb, is allowed to leave the system. We use a continuous degassing process, in which the rate of ^3He loss is constant at each case and $^3\text{He}/^4\text{He}$ is not fractionated during degassing. $^{207}\text{Pb}^*/^{206}\text{Pb}^*$ is the ratio of radiogenic ingrowth of ^{207}Pb and ^{206}Pb since the formation of the Earth²¹, and is defined as $^{207}\text{Pb}^*/^{206}\text{Pb}^* = (^{207}\text{Pb}/^{204}\text{Pb} - 10.297)/(^{206}\text{Pb}/^{204}\text{Pb} - 9.307)$. The percentages labeled in **Panel c** are the present-day ^3He budget left in each partially degassed primitive mantle reservoir, and the 100% model line represents the undegassed primitive mantle. The calculation was done step-wisely with a step of 10 Ma, and the details are in Table S1. The two horizontal trends in **Panel c** label the present-day average MORB $^3\text{He}/^4\text{He}$ value (8 R/Ra) and the highest $^3\text{He}/^4\text{He}$ observed (50 R/Ra).

$^{206}\text{Pb}/^{204}\text{Pb}$ – $^3\text{He}/^4\text{He}$ and positive $^{207}\text{Pb}^*/^{206}\text{Pb}^*$ – $^3\text{He}/^4\text{He}$ trends, with the high $^3\text{He}/^4\text{He}$ associated with ancient Pb isotopic signature, i.e., low $^{206}\text{Pb}/^{204}\text{Pb}$ and high $^{207}\text{Pb}^*/^{206}\text{Pb}^*$ (Figs. 1, 2b, 2c). We note that due to crustal contamination or post-eruptive radiogenic ingrowth of ^4He , the average $^3\text{He}/^4\text{He}$ for each OIB-CFB suite likely represents a minimum bound on the isotopic signature of the primary magma. Thus, a more informative approach is to plot the maximum observed $^3\text{He}/^4\text{He}$ at each OIB-CFB suite. As shown in Figs. 2d and 2e, maximum observed values also form negative $^{206}\text{Pb}/^{204}\text{Pb}$ – $^3\text{He}/^4\text{He}$ and positive $^{207}\text{Pb}^*/^{206}\text{Pb}^*$ – $^3\text{He}/^4\text{He}$ trends, implying that such correlations are mantle signatures.

High $^3\text{He}/^4\text{He}$ is usually explained as a signature of undegassed and unprocessed mantle. For example, Jackson et al.³⁹ observed that high $^3\text{He}/^4\text{He}$ is associated with ancient Pb isotopic signature in Baffin Island and West Greenland lavas, and they proposed that this reflects sampling of undegassed primitive mantle. Recently, alternative views have entertained the possibility that high $^3\text{He}/^4\text{He}$ might instead reflect ancient residues of mantle melting owing to preferential partitioning of U relative to He into the melt³¹, but it is not clear how such a scenario would affect time-integrated Pb isotopes. Sulfide-rich cumulates formed during the formation of continental crust early in the Earth's history¹³ would be characterized by low $^{206}\text{Pb}/^{204}\text{Pb}$ and high $^3\text{He}/^4\text{He}$ and $^{207}\text{Pb}^*/^{206}\text{Pb}^*$ as discussed above (Figs. 1, 2). The great majority of these cumulates are thought to have delaminated back into the mantle or been stored as small pockets within the continental lithosphere¹³. If these cumulates are tapped by plumes, by small scale convective instabilities or are preferentially melted during lithospheric heating/extension, the coupled Pb-He isotopic systematics would emerge in OIB systematics as can be seen in Figure 2. These signatures would not be expected to appear in mid-ocean ridge basalts because the higher extents of melting beneath ridges would dilute the pyroxenite signature by the signature of ambient mantle.

If ancient sulfide-bearing cumulates exist in the convecting mantle or continental lithospheric mantle, we might expect to see coupled Pb-He signatures in continental intraplate magmas as well. One of the few continental intraplate localities that have been extensively studied in terms of Pb and He isotopic systematics is the Yellowstone-Snake River Plain basalts. From east to west, Yellowstone, Snake River Plain, Owyhee Plateau and the Oregon High Lava Plains (Fig. 3) are thought to reflect a continental hotspot track formed by the Yellowstone plume⁴⁰. Snake River Plain lavas have high $^3\text{He}/^4\text{He}$ (Fig. 3), typical of OIBs, which were used to support a mantle plume origin for these lavas^{40–42}. We note, however, that $^3\text{He}/^4\text{He}$ and $^{207}\text{Pb}^*/^{206}\text{Pb}^*$ increase and $^{206}\text{Pb}/^{204}\text{Pb}$ decreases from west to east along this hotspot track⁴² (Fig. 3), indicating that $^3\text{He}/^4\text{He}$ is positively correlated with $^{207}\text{Pb}^*/^{206}\text{Pb}^*$ and negatively correlated with $^{206}\text{Pb}/^{204}\text{Pb}$, just as in the global OIB-CFB dataset (Fig. 2). Snake River Plain lavas with high $^3\text{He}/^4\text{He}$, $^{207}\text{Pb}^*/^{206}\text{Pb}^*$ and low $^{206}\text{Pb}/^{204}\text{Pb}$ were emplaced through Precambrian North American Craton, while the High Lava Plains lavas with low $^3\text{He}/^4\text{He}$, $^{207}\text{Pb}^*/^{206}\text{Pb}^*$ and high $^{206}\text{Pb}/^{204}\text{Pb}$ were emplaced through Mesozoic accreted terrains. Although these spatio-temporal trends have been interpreted to represent changes in the dynamics of plume-lithosphere interactions^{40–42}, the close adherence of these isotopic patterns to basement geology and age suggests that the Pb and He isotopic systematics may in fact be derived from the North American lithosphere and that the isotopic variations reflect variations in the age of the Pb and He sources. A simple way of generating such systematics is to tap an ancient sulfide-bearing reservoir in the cratonic part of the Yellowstone-Snake River Plain volcanic series.

In summary, the negative $^3\text{He}/^4\text{He}$ – $^{206}\text{Pb}/^{204}\text{Pb}$ and positive $^3\text{He}/^4\text{He}$ – $^{207}\text{Pb}^*/^{206}\text{Pb}^*$ trends in global OIB-CFBs and in continental intraplate magmas require a reservoir characterized by low time-integrated U/Pb and U/He, resulting in unradiogenic Pb and He isotopic signatures. Unradiogenic He is traditionally interpreted to represent an undegassed and hence primitive, unprocessed reservoir. Here, we suggest that the unradiogenic Pb (low $^{206}\text{Pb}/^{204}\text{Pb}$ and high $^{207}\text{Pb}^*/^{206}\text{Pb}^*$) and He isotopic signatures represent ancient mantle signatures frozen in the form of sulfide liquids co-precipitated with large masses of mafic cumulates (pyroxenites) during major melting events associated with the formation of continents. In this regard, the $^3\text{He}/^4\text{He}$ isotopic signature of the mantle may reflect the integrated effect of major crust-forming events, as argued by Parman⁴³ but for different reasons. The reason why most of the upper mantle and continental crust is more radiogenic than the bulk Earth is thus because there exists a large reservoir of mafic, sulfide-bearing cumulates now stored in the mantle or deep lithosphere and complement-

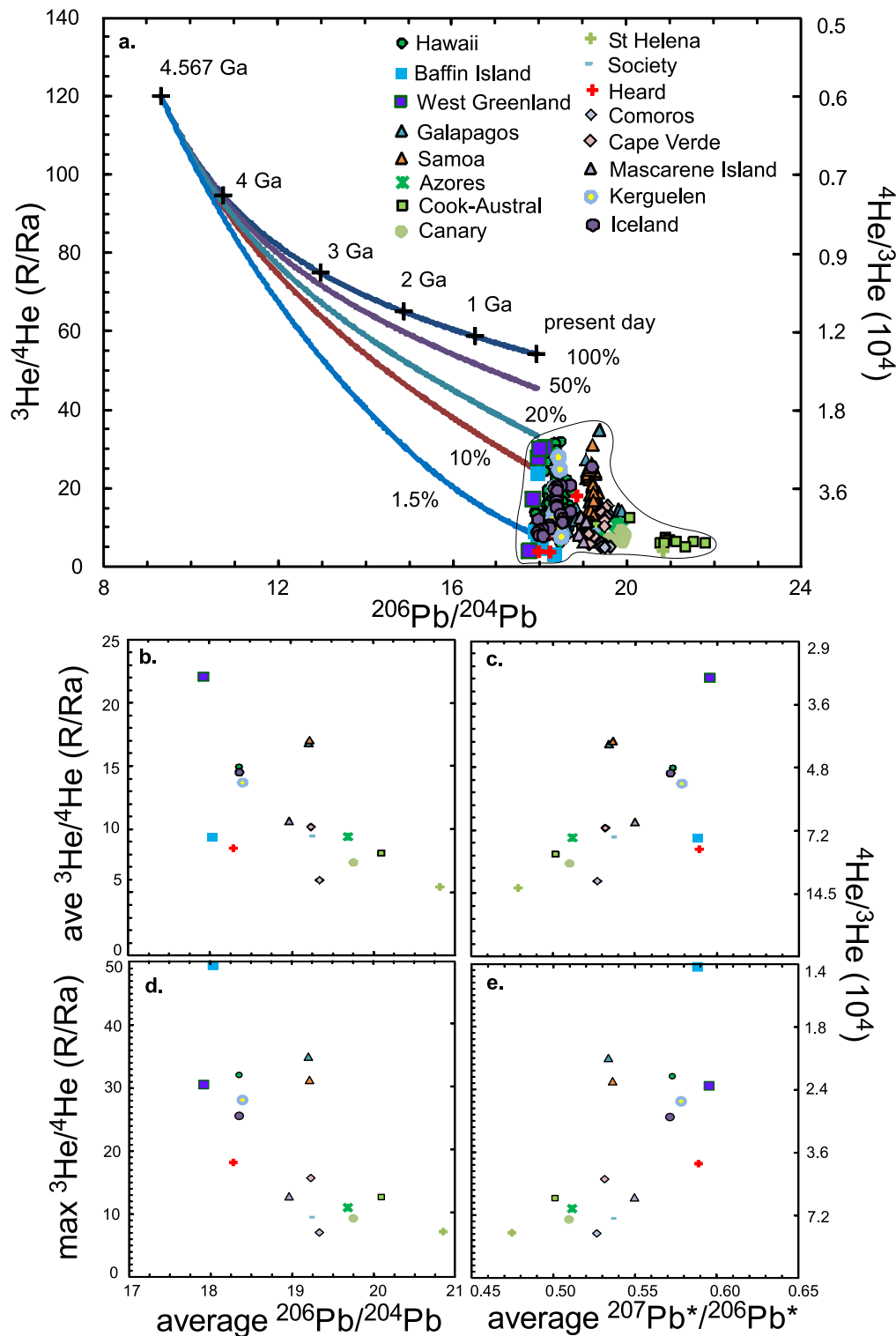


Figure 2 | (a) $^{206}\text{Pb}/^{204}\text{Pb}$ vs. $^3\text{He}/^4\text{He}$ for sulfides formed at different ages and ocean island basalts (OIBs) and continental flood basalts (CFBs). Lines are cross plots of $^{206}\text{Pb}/^{204}\text{Pb}$ vs. $^3\text{He}/^4\text{He}$ for sulfides formed at different ages as modeled in Fig. 1. Since sulfides have very low U/Pb and (U + Th)/He ratios, they preserve the mantle $^{206}\text{Pb}/^{204}\text{Pb}$, $^{207}\text{Pb}^*/^{206}\text{Pb}^*$ and $^3\text{He}/^4\text{He}$ signatures at the time when they formed. In OIBs, the high $^3\text{He}/^4\text{He}$ is associated with low $^{206}\text{Pb}/^{204}\text{Pb}$. (b) and (c) $^{206}\text{Pb}/^{204}\text{Pb}$ and $^{207}\text{Pb}^*/^{206}\text{Pb}^*$ vs. $^3\text{He}/^4\text{He}$ for the average of each OIB-CFB suite. No age-corrections were applied to $^3\text{He}/^4\text{He}$ of Baffin Island and West Greenland. Consequently the plotted $^3\text{He}/^4\text{He}$ are their minimal values. (d) and (e) average $^{206}\text{Pb}/^{204}\text{Pb}$ and $^{207}\text{Pb}^*/^{206}\text{Pb}^*$ vs. maximum $^3\text{He}/^4\text{He}$ of each OIB-CFB suite. Data are downloaded from GeoRoc database, and are in Table S2.

ary to the continental crust today. Most recently, it has been suggested that amphiboles might serve as potential reservoirs of He and other noble gases⁴⁴. While this may be true, the stability field of amphiboles in the mantle is rather limited and, without sulfide, there

is no obvious connection with Pb. We conclude that sulfide-bearing lithologies provide the most internally consistent explanation for the coupled Pb-He isotopic systematics of major mantle and crustal reservoirs. In particular, Pb and He isotopic systematics of the mantle

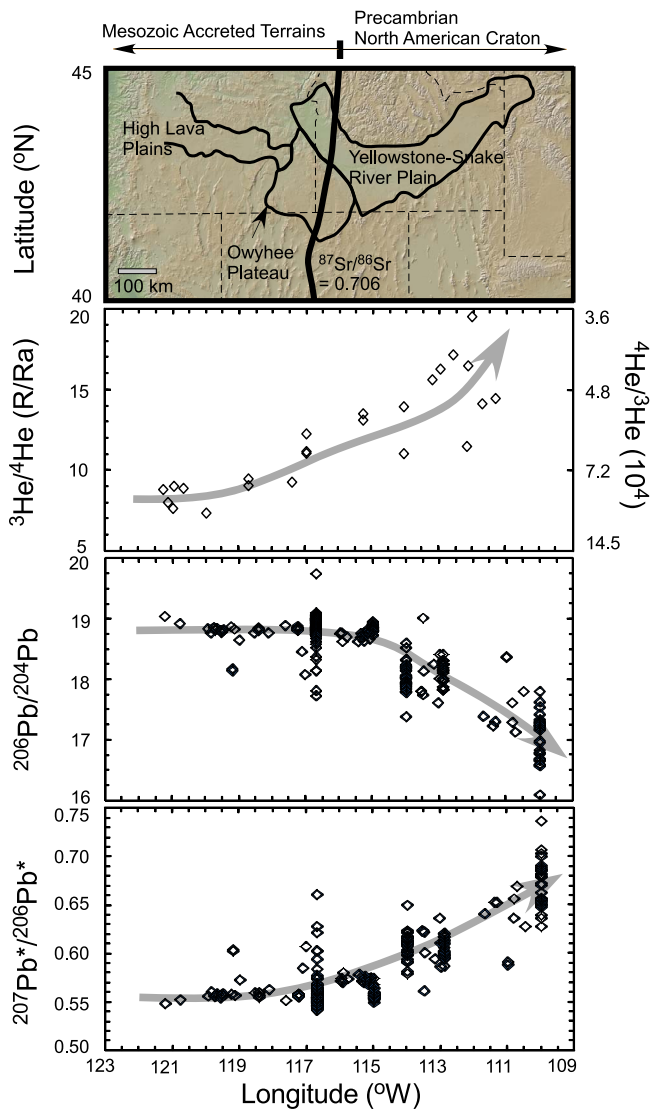


Figure 3 | $^{206}\text{Pb}/^{204}\text{Pb}$, $^{207}\text{Pb}^*/^{206}\text{Pb}^*$ and $^3\text{He}/^4\text{He}$ vs. longitude relationship for basalts from Northwestern United States. The high $^3\text{He}/^4\text{He}$ is associated with low $^{206}\text{Pb}/^{204}\text{Pb}$. The $^{87}\text{Sr}/^{86}\text{Sr} = 0.706$ line is used to label the boundary of North American Craton. Map is generated using GeoMapApp, and the distributions of basalts follow Graham et al.⁴². Data are downloaded from GeoRoc database, and are in Table S3.

reflect the integrated production and destruction of continents rather than the preservation of primordial, unprocessed parcels of mantle that have survived unscathed throughout Earth's history. It is thus worth exploring the role of sulfides during silicate differentiation of the Earth, and in this regard, it may be worth examining the impact of sulfides on the geochemical signatures of mantle-derived magmas through time. However, because S contents in magmas are controlled by sulfide solubility and the formation of cumulates occurs at high temperatures, the impact of sulfides is not likely to be easily studied by S content or S isotopes in magmas. A more fruitful approach would be to investigate the secular evolution of chalcophile elements, such as Cu, Ag, Pt and Pd, in the mantle as the behaviors of these elements during melting are strongly influenced by the presence of sulfides.

1. Allegre, C. J. Behavior of Uranium-Thorium-Lead Systems in Upper Mantle and Model of Mantle Development during Geological Times. *Earth Planet Sci Lett* **5**, 261–269, doi: 10.1016/S0012-821X(68)80050-0 (1968).

2. O'Nions, R. K., Evensen, N. M. & Hamilton, P. J. Geochemical modeling of mantle differentiation and crustal growth. *J Geophys Res* **84**, 6091–6101, doi:10.1029/JB084iB11p06091 (1979).
3. Rudnick, R. L. & Goldstein, S. L. The Pb isotopic compositions of lower crustal xenoliths and the evolution of lower crustal Pb. *Earth Planet Sci Lett* **98**, 192–207, doi:10.1016/0012-821X(90)90059-7 (1990).
4. Zartman, R. E. & Haines, S. M. The Plumbotectonic Model for Pb Isotopic Systematics among Major Terrestrial Reservoirs - a Case for Bi-Directional Transport. *Geochim Cosmochim Acta* **52**, 1327–1339, doi:10.1016/0016-7037(88)90204-9 (1988).
5. Rudnick, R. L. & Gao, S. Composition of the Continental Crust. *Treatise on Geochemistry* 3. Editor: Roberta L. Rudnick. Executive Editors: Heinrich D. Holland and Karl K. Turekian. ISBN 0-08-043751-6. 1–64, doi:10.1016/b0-08-043751-6/03016-4 (Elsevier 2003).
6. Wood, B. J. & Halliday, A. N. The lead isotopic age of the Earth can be explained by core formation alone. *Nature* **465**, 767–770, doi:10.1038/Nature09072 (2010).
7. Allegre, C. J., Manhès, G. & Gopel, C. The Age of the Earth. *Geochim Cosmochim Acta* **59**, 1445–1456, doi:10.1016/0016-7037(95)00054-4 (1995).
8. Kleine, T., Munker, C., Mezger, K. & Palme, H. Rapid accretion and early core formation on asteroids and the terrestrial planets from Hf-W chronometry. *Nature* **418**, 952–955, doi:10.1038/Nature0982 (2002).
9. Yin, Q. Z. et al. A short timescale for terrestrial planet formation from Hf-W chronometry of meteorites. *Nature* **418**, 949–952, doi:10.1038/Nature0995 (2002).
10. Albarède, F. Volatile accretion history of the terrestrial planets and dynamic implications. *Nature* **461**, 1227–1233, doi:10.1038/Nature08477 (2009).
11. Galer, S. J. G. & Goldstein, S. L. Influence of accretion on lead in the Earth. *Earth Processes: Reading the Isotopic Code* Editor: Basu, A. & Hart, S. R. *Geophys Monogra* **95**, 75–98 (AGU 1996).
12. Hart, S. R. & Gaetani, G. A. Mantle Pb paradoxes: the sulfide solution. *Contrib Mineral Petrol* **152**, 295–308, doi:10.1007/s00410-006-0108-1 (2006).
13. Lee, C.-T. A. et al. Copper Systematics in Arc Magmas and Implications for Crust-Mantle Differentiation. *Science* **336**, 64–68, doi:10.1126/science.1217313 (2012).
14. Kay, R. W. & Kay, S. M. Crustal Recycling and the Aleutian Arc. *Geochim Cosmochim Acta* **52**, 1351–1359, doi:10.1016/0016-7037(88)90206-2 (1988).
15. Lee, C. T. A., Morton, D. M., Kistler, R. W. & Baird, A. K. Petrology and tectonics of Phanerozoic continent formation: From island arcs to accretion and continental arc magmatism. *Earth Planet Sci Lett* **263**, 370–387, doi:10.1016/j.epsl.2007.09.025 (2007).
16. Metrich, N. & Mandeville, C. W. Sulfur in Magmas. *Elements* **6**, 81–86, doi:10.2113/gselements.6.2.81 (2010).
17. Sharma, K., Blake, S., Self, S. & Krueger, A. J. SO₂ emissions from basaltic eruptions, and the excess sulfur issue. *Geophys Res Lett* **31**, L13612, doi:10.1029/2004gl019688 (2004).
18. Wallace, P. J. Volatiles in subduction zone magmas: concentrations and fluxes based on melt inclusion and volcanic gas data. *J Volcanol Geoth Res* **140**, 217–240, doi:10.1016/j.jvolgeores.2004.07.023 (2005).
19. Burton, K. W. et al. Unradiogenic lead in Earth's upper mantle. *Nat Geosci* **5**, 570–573, doi:10.1038/ngeo1531 (2012).
20. Mungall, J. E. & Su, S. G. Interfacial tension between magmatic sulfide and silicate liquids: Constraints on kinetics of sulfide liquation and sulfide migration through silicate rocks. *Earth Planet Sci Lett* **234**, 135–149, doi:10.1016/j.epsl.2005.02.035 (2005).
21. Galer, S. J. G. & Onions, R. K. Residence Time of Thorium, Uranium and Lead in the Mantle with Implications for Mantle Convection. *Nature* **316**, 778–782, doi:10.1038/316778a0 (1985).
22. Yang, J. & Anders, E. Sorption of Noble-Gases by Solids, with Reference to Meteorites. 3. Sulfides, Spinels, and Other Substances - on the Origin of Planetary Gases. *Geochim Cosmochim Acta* **46**, 877–892, doi:10.1016/0016-7037(82)90044-8 (1982).
23. Jambon, A., Weber, H. & Braun, O. Solubility of He, Ne, Ar, Kr and Xe in a Basalt Melt in the Range 1250–1600-Degrees-C. *Geochim Cosmochim Acta* **50**, 401–408, doi:10.1016/0016-7037(86)90193-6 (1986).
24. Lux, G. The Behavior of Noble-Gases in Silicate Liquids - Solution, Diffusion, Bubbles and Surface Effects, with Applications to Natural Samples. *Geochim Cosmochim Acta* **51**, 1549–1560, doi:10.1016/0016-7037(87)90336-X (1987).
25. Carroll, M. R. & Stolper, E. M. Noble-Gas Solubilities in Silicate Melts and Glasses - New Experimental Results for Argon and the Relationship between Solubility and Ionic Porosity. *Geochim Cosmochim Acta* **57**, 5039–5051, doi:10.1016/0016-7037(93)90606-W (1993).
26. Uhlig, H. H. The solubilities of gases and surface tension. *J Phys Chem-US* **41**, 1215–1225, doi:10.1021/J150387a007 (1937).
27. Blander, M., Grimes, W. R., Smith, N. V. & Watson, G. M. Solubility of Noble Gases in Molten Fluorides. 2. In the LiF-NaF-KF Eutectic Mixture. *J Phys Chem-US* **63**, 1164–1167, doi:10.1021/J150577a033 (1959).
28. Zhang, Y. X. & Xu, Z. J. Atomic Radii of Noble-Gas Elements in Condensed Phases. *Am Mineral* **80**, 670–675 (1995).
29. Walker, D. & Mullins, O. Surface-Tension of Natural Silicate Melts from 1,200-Degrees-C-1,500-Degrees-C and Implications for Melt Structure. *Contrib Mineral Petrol* **76**, 455–462, doi:10.1007/Bf00371487 (1981).



30. Gaetani, G. A. & Grove, T. L. Wetting of mantle olivine by sulfide melt: implications for Re/Os ratios in mantle peridotite and late-stage core formation. *Earth Planet Sci Lett* **169**, 147–163, doi:10.1016/S0012-821x(99)00062-X (1999).
31. Parman, S. W., Kurz, M. D., Hart, S. R. & Grove, T. L. Helium solubility in olivine and implications for high $^3\text{He}/^4\text{He}$ in ocean island basalts. *Nature* **437**, 1140–1143, doi:10.1038/Nature04215 (2005).
32. Graham, D. W. Noble gas isotope geochemistry of mid-ocean ridge and ocean island basalts: Characterization of mantle source reservoirs. *Rev Mineral Geochem* **47**, 247–317, doi:10.2138/rmg.2002.47.8 (2002).
33. Stuart, F. M., Lass-Evans, S., Fitton, J. G. & Ellam, R. M. High $^3\text{He}/^4\text{He}$ ratios in picritic basalts from Baffin Island and the role of a mixed reservoir in mantle plumes. *Nature* **424**, 57–59, doi:10.1038/Nature01711 (2003).
34. Lee, C. T. A. *et al.* Upside-down differentiation and generation of a ‘primordial’ lower mantle. *Nature* **463**, 930–933, doi:10.1038/Nature08824 (2010).
35. Jackson, M. G., Kurz, M. D., Hart, S. R. & Workman, R. K. New Samoan lavas from Ofu Island reveal a hemispherically heterogeneous high $^3\text{He}/^4\text{He}$ mantle. *Earth Planet Sci Lett* **264**, 360–374, doi:10.1016/j.epsl.2007.09.023 (2007).
36. Class, C. & Goldstein, S. L. Evolution of helium isotopes in the Earth’s mantle. *Nature* **436**, 1107–1112, doi:10.1038/Nature03930 (2005).
37. Porcelli, D. & Elliott, T. The evolution of He Isotopes in the convecting mantle and the preservation of high $^3\text{He}/^4\text{He}$ ratios. *Earth Planet Sci Lett* **269**, 175–185, doi:10.1016/j.epsl.2008.02.002 (2008).
38. Gonnermann, H. M. & Mukhopadhyay, S. Non-equilibrium degassing and a primordial source for helium in ocean-island volcanism. *Nature* **449**, 1037–1040, doi:10.1038/Nature06240 (2007).
39. Jackson, M. G. *et al.* Evidence for the survival of the oldest terrestrial mantle reservoir. *Nature* **466**, 853–856, doi:10.1038/Nature09287 (2010).
40. Hanan, B. B., Shervais, J. W. & Vetter, S. K. Yellowstone plume-continental lithosphere interaction beneath the Snake River Plain. *Geology* **36**, 51–54, doi:10.1130/G23935a.1 (2008).
41. Craig, H., Lupton, J. E., Welhan, J. A. & Poreda, R. Helium Isotope Ratios in Yellowstone Park and Lassen Park Volcanic Gases. *Geophys Res Lett* **5**, 897–900, doi:10.1029/Gl005i011p00897 (1978).
42. Graham, D. W. *et al.* Mantle source provinces beneath the Northwestern USA delimited by helium isotopes in young basalts. *J Volcanol Geoth Res* **188**, 128–140, doi:10.1016/j.jvolgeores.2008.12.004 (2009).
43. Parman, S. W. Helium isotopic evidence for episodic mantle melting and crustal growth. *Nature* **446**, 900–903, doi:10.1038/Nature05691 (2007).
44. Jackson, C. R. M., Parman, S., Kelley, S. P. & Cooper, R. F. Noble gas transport into the mantle facilitated by high solubility in amphibole. *Nat Geosci* **6**, 562–565, doi:10.1038/Ngeo1851 (2013).

Acknowledgments

This work was supported in part by NSF grants EAR 1119315 to CTL and EAR 1144727 to SH, and a NASA grant NNX11AJ51G to QZY.

Author contributions

S.H., C.T.L. and Q.Z.Y. wrote the main manuscript text, and prepared figures 1–3. All authors reviewed the manuscript.

Additional information

Supplementary information accompanies this paper at <http://www.nature.com/scientificreports>

Competing financial interests: The authors declare no competing financial interests.

How to cite this article: Huang, S.C., Lee, C.-T.A. & Yin, Q.-Z. Missing Lead and High $^3\text{He}/^4\text{He}$ in Ancient Sulfides Associated with Continental Crust Formation. *Sci. Rep.* **4**, 5314; DOI:10.1038/srep05314 (2014).



This work is licensed under a Creative Commons Attribution-NonCommercial-NoDerivs 4.0 International License. The images or other third party material in this article are included in the article’s Creative Commons license, unless indicated otherwise in the credit line; if the material is not included under the Creative Commons license, users will need to obtain permission from the license holder in order to reproduce the material. To view a copy of this license, visit <http://creativecommons.org/licenses/by-nc-nd/4.0/>